Article:

Ng, B.K., David, J.P.R., Tozer, R.C. et al. (4 more authors) (2003) Nonlocal effects in thin 4H-SiC UV avalanche photodiodes. IEEE Transactions on Electron Devices, 50 (8). pp. 1724-1732. ISSN 0018-9383

https://doi.org/10.1109/TED.2003.815144

Nonlocal Effects in Thin 4H-SiC UV Avalanche Photodiodes

B. K. Ng, John P. R. David, *Senior Member, IEEE*, Richard C. Tozer, *Senior Member, IEEE*, Graham J. Rees, Feng Yan, *Senior Member, IEEE*, Jian H. Zhao, *Senior Member, IEEE*, and Maurice Weiner, *Fellow, IEEE*

***Abstract*—The avalanche multiplication and excess noise characteristics of 4H-SiC avalanche photodiodes with i-region widths of 0.105 and 0.285 μm have been investigated using 230–365-nm light, while the responsivities of the photodiodes at unity gain were examined for wavelengths up to 375 nm. Peak unity gain responsivities of more than 130 mA/W at 265 nm, equivalent to quantum efficiencies of more than 60%, were obtained for both structures. The measured avalanche characteristics show that $\beta > \alpha$ and that the β/α ratio remains large even in thin 4H-SiC avalanche regions. Very low excess noise, corresponding to $k_{eff} < 0.15$ in the local noise model, where $k_{eff} = \alpha/\beta(\beta/\alpha)$ for hole (electron) injection, was measured with 365-nm light in both structures. Modeling the experimental results using a simple quantum efficiency model and a nonlocal description yields effective ionization threshold energies of 12 and 8 eV for electrons and holes, respectively, and suggests that the dead space in 4H-SiC is soft. Although dead space is important, pure hole injection is still required to ensure low excess noise in thin 4H-SiC APDs owing to β/α ratios that remain large, even at very high fields.**

***Index Terms*—Avalanche multiplication, avalanche photodiodes (APDs), breakdown voltage, dead space, impact ionization, ionization coefficients, nonlocal effects.**

I. Introduction

Silicon carbide (SiC) and III-nitrides are promising materials for ultraviolet (UV) sensing owing to their wide band gaps. Photodiodes utilizing these wide band-gap materials have the potential to operate at high temperature with low leakage current and good visible-blind/solar-blind performance. Avalanche photodiodes (APDs) with thin avalanche widths can greatly enhance the signal-to-noise ratio (SNR) of optical receivers limited by weak optical signals and high amplifier noise by providing internal gain, while maintaining high operating speeds and low operating voltages. The realization of III-nitride APDs is currently limited by material issues due to the lack of a native nitride substrate, although there has been some success in the demonstration of GaN APDs [1], [2] from using small device areas to achieve microplasma-free performance. By contrast, SiC is technologically more mature and is a potential alternative to the III-nitrides for UV detection. The 4H polytype of SiC has, in addition to its superior thermophysical properties, the advantage of widely differing ionization coefficients [3] for electrons (α) and holes (β), which is crucial for realising APDs with low excess avalanche noise [4]. We have recently demonstrated very low noise UV APDs based on a 0.1-μm 4H-SiC avalanche region and showed unambiguously that $\beta > \alpha$ in 4H-SiC from multiplication measurements [5]. In addition, our results suggest that dead space, the distance over which the ionization coefficient reaches equilibrium with the electric field, may occupy a significant fraction of the avalanche width of 4H-SiC APDs. It is therefore necessary to examine the effect of dead space on the avalanche characteristics of 4H-SiC since such knowledge is crucial for the design and optimization of APDs employing thin avalanche regions. Furthermore, the discrepancy between the published experimental values of β for 4H-SiC by Konstantinov *et al.* [3] and Raghunathan and Baliga [6] merits further investigation. The accurate determination of the impact ionization coefficients in 4H-SiC has direct application to the design and optimization of high-temperature, high-power and high-frequency devices.

This paper investigates nonlocal impact ionization effects in thin 4H-SiC devices using two APD structures with nominal avalanche widths of 0.1 and 0.2 μm. The experimental details of this paper are described in Section II. Section III reports the responsivity and the avalanche multiplication characteristics of the APDs obtained from measurements. In Section IV, the measurements are interpreted using a simple quantum efficiency model and a nonlocal multiplication model. The modeled results are also discussed and compared with previous works in Section IV, and the conclusions of this paper are summarized in Section V.

II. Experiment

A. Layer Details

The APD structure with avalanche width of $w = 0.1$ μm has been reported in [5] and comprises a 2-μm n layer, a 0.1-μm i region, a 0.2-μm p layer, and a thin 0.1-μm p^+ cap grown on n^+4H-SiC substrate [inset of Fig. 1(a)]. The other APD structure has a reach-through layer to increase the quantum efficiency of penetrating UV light and is made up of a 2-μm n^- reach-through layer, a 0.11 μm n layer, a 0.2-μm i-region, a 0.25-μm p layer and a 0.2-μm p^+ cap grown on an n^+substrate [inset of Fig. 1(b)]. The intended doping levels were 4×10^{15},

Manuscript received January 2, 2003. This work was supported in part by EPSRC (U.K.). The review of this paper was arranged by Editor C.-P. Lee.

B. K. Ng was with the Department of Electronic and Electrical Engineering, University of Sheffield, Sheffield, S1 3JD, U.K. He is now with the Department of Electrical and Electronic Engineering, Nanyang Technological University, Singapore 639798 (e-mail: ebkng@ntu.edu.sg).

J. P. R. David, R. C. Tozer, and G. J. Rees are with the Department of Electronic and Electrical Engineering, University of Sheffield, Sheffield, S1 3JD U.K. (e-mail: j.p.david@sheffield.ac.uk).

F. Yan and J. H. Zhao are with the Department of Electrical and Computer Engineering, Rutgers University, Piscataway, NJ 08540 USA.

M. Weiner is with the United Silicon Carbide, Inc., North Brunswick, NJ 08901 USA.

Digital Object Identifier 10.1109/TED.2003.815144

1×10^{18}, 1.3×10^{18}, and $3 \times 10^{19}\ \mathrm{cm}^{-3}$ for the n$^-$, n, p, and p$^+$ layers, respectively, of the second structure.

Square mesa diodes with areas ranging from $60 \times 60\ \mu\mathrm{m}^2$ to $210 \times 210\ \mu\mathrm{m}^2$ were fabricated using a 2° positive bevel edge termination technology [7] for the first APD structure. The reach-through APD structure was fabricated using a multistep junction extension termination [8] to create $50 \times 50\ \mu\mathrm{m}^2$ to $200 \times 200\ \mu\mathrm{m}^2$ mesa diodes. Windows were formed on the top ohmic contacts to provide optical access and thin layers of $\mathrm{SiO_2/Si_3N_4}$ and $\mathrm{SiO_2}$ were used to passivate the beveled APDs (BAPDs) and the multistep junction extension terminated APDs (MAPDs), respectively. The width and average doping level of the i-region of the BAPDs are found to be 0.1 μm and $1.5 \times 10^{17}\ \mathrm{cm}^{-3}$ p-type, respectively, from secondary ion mass spectroscopy (SIMS) measurement. The SIMS profile indicates that the doping levels in the cladding layers adjacent to the i-region are $2 \sim 3 \times 10^{18}\ \mathrm{cm}^{-3}$.

Fig. 1(a) and (b) shows the measured and modeled capacitance–voltage (*C–V*) profiles of $210 \times 210\ \mu\mathrm{m}^2$ BAPDs and $200 \times 200\ \mu\mathrm{m}^2$ MAPDs, respectively. The *C–V* profile of the MAPDs indicates that the 2 $\mu\mathrm{m}$ n$^-$ reach-through layer is not depleted, even when the bias approaches the breakdown voltage V_{bd}. *C–V* modeling from solving Poisson's equation within the depletion approximation and assuming p-i-n structures gave $w = 0.105\ \mu\mathrm{m}$ and $w = 0.285\ \mu\mathrm{m}$ for the BAPDs and the MAPDs, respectively. The doping levels in the i-region of the BAPDs and the MAPDs are estimated to be $1.25 \times 10^{17}\ \mathrm{cm}^{-3}$ and $8.11 \times 10^{15}\ \mathrm{cm}^{-3}$, respectively, while the doping levels in the cladding layers of both structures have values of $1 \sim 3 \times 10^{18}\ \mathrm{cm}^{-3}$. The parameters extracted from the *C–V* characteristics of the BAPDs are found to be in good agreement with those determined from SIMS measurement. The diffusion voltage was estimated to be 2.9 V from extrapolating the *C–V* measurements and is consistent with the value calculated using the data of Henning *et al.* [9].

Reverse dark current–voltage (*I–V*) measurements indicate that the breakdowns are sharp and the reverse dark current is observed to increase by several orders of magnitude at the breakdown voltage. The breakdown voltages estimated from dark *I–V* measurements are 58.5 and 124.0 V for the BAPDs and the MAPDs, respectively. Most diodes exhibit low dark currents prior to breakdown and the average dark current density of the BAPDs and the MAPDs at 95% V_{bd} are 8 and 7 $\mu\mathrm{A/cm^2}$, respectively. Forward *I–V* measurements indicate that series resistance is negligible over the current range measured.

B. Measurement Techniques

The spectral response of the diodes was measured using a mercury–xenon (Hg–Xe) lamp, a 0.22-m monochromator and a lock-in amplifier. The output beam from the monochromator was modulated at 180 Hz with a mechanical chopper and was focussed onto the optical window of the largest diodes. The absolute spectral responsivity of the diodes was obtained by calibrating the optical system with a commercial UV-enhanced Si photodiode.

The multiplication characteristics of the APDs under different carrier injection conditions were investigated using UV light from the Hg-Xe lamp and a HeCd laser. Photogenerated carriers were injected into the high field region of the diodes by focussing 230–365-nm light from the Hg-Xe lamp or 325-nm light from the HeCd laser to a small spot ($\sim 120 \times 80\ \mu\mathrm{m}^2$ and $\sim 10\ \mu\mathrm{m}$ diameter, respectively) onto the optical access windows. DC photocurrents were measured as a function of reverse bias voltage with a source-measure unit. To confirm the dc results, phase-sensitive ac measurements were also taken on some diodes using a lock-in amplifier and modulated UV light. Photocurrents as low as 10 nA were unambiguously measured using the phase-sensitive detection technique.

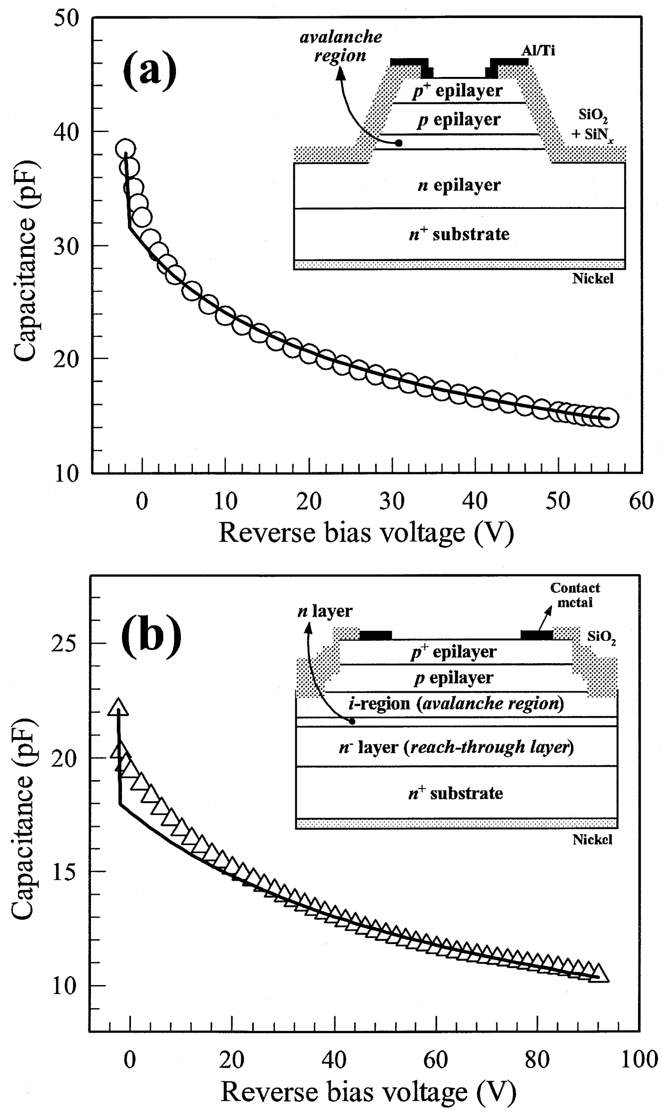

Fig. 1. Measured (symbols) and modeled (lines) *C–V* characteristics of the (a) BAPDs and the (b) MAPDs with device areas of $210 \times 210\ \mu\mathrm{m}^2$ and $200 \times 200\ \mu\mathrm{m}^2$, respectively. The schematic view of the APD structures are depicted in the insets.

The multiplication factor M was obtained by normalizing the measured photocurrent to the primary photocurrent linearly extrapolated from the measured photocurrent at low bias. The multiplication characteristics from both dc and ac measurements were found to be indistinguishable. Gain uniformity of the layers was confirmed by measurement of identical multiplication characteristics on several diodes across the wafer. Multiplication values in excess of 200 were achieved for both structures. It was noted that the reverse bias photocurrent characteristic of the MAPDs did not exhibit the "step" characteristic of reach-through

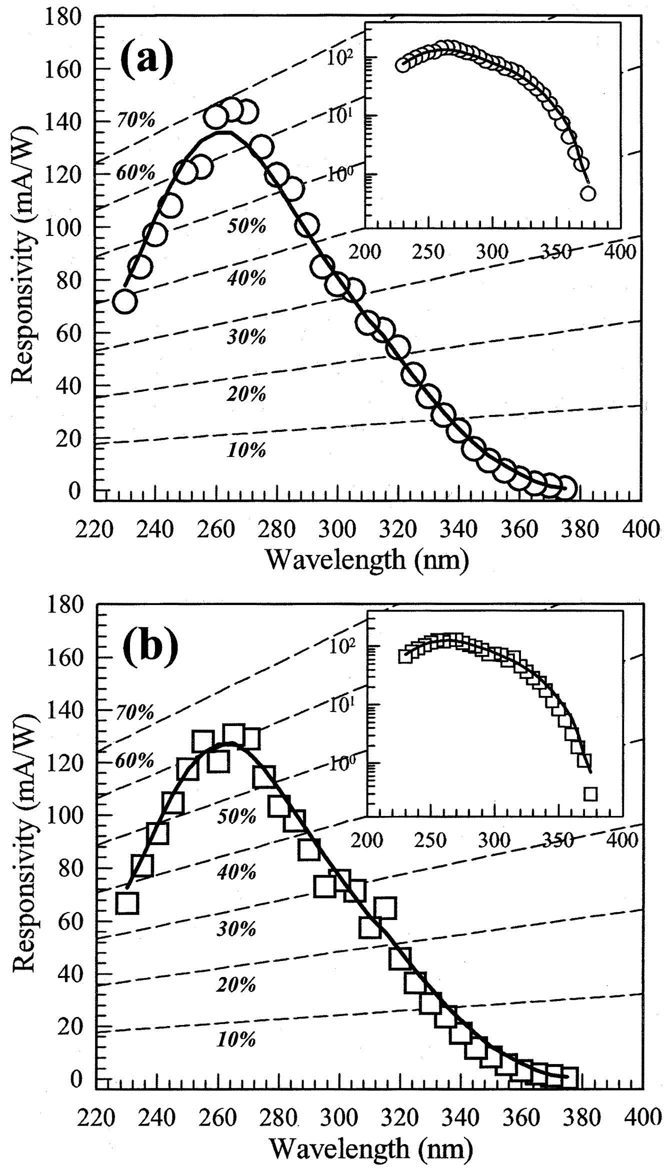

Fig. 2. Typical unity gain spectral responsivities of the (a) BAPDs (○) and the (b) MAPDs (□) over the wavelength range 230–375 nm. The responsivity curves (dashed lines) corresponding to external quantum efficiency of 10 to 70% are also included for reference. The insets show the same curves on semilogarithmic plots. Modeled results are shown as solid lines.

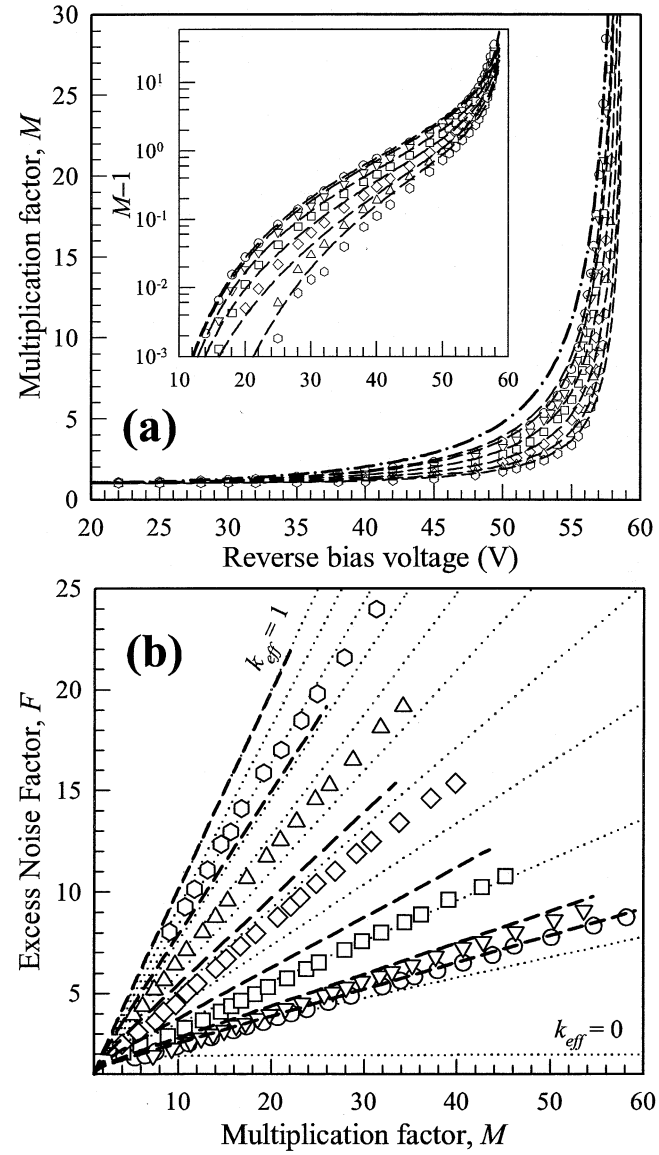

Fig. 3. Measured (symbols) and modeled (dashed lines) (a) multiplication and (b) excess noise characteristics of the BAPD structure from 230 nm (hexagon), 240 nm (△), 250 nm (◇), 265 nm (□), 297 nm (▽), and 365 nm (○). Inset in (a) shows $(M - 1)$ plotted on a logarithmic scale to accentuate the low multiplication values. The modeled M_h (dot-dashed line) is also shown in (a) for comparison. Dotted lines in (b) are McIntyre's local prediction for $k_{\text{eff}} = 0$ to 1 in steps of 0.1.

photodiodes when illuminated with weakly absorbed light. This indicates that there is no significant discontinuity in the quantum efficiency with bias and confirms that the 2 μm n^- layer of the MAPDs is not depleted up to device breakdown. The excess noise factor F was also measured at a center frequency of 10 MHz and a noise effective bandwidth of 4.2 MHz using the phase-sensitive detection technique and the measurement system of Li *et al.* [10]. As before, several diodes across each layer were measured to ensure reproducibility.

III. Experimental Results

The typical unity gain spectral responsivity curves of the BAPDs and the MAPDs are shown in Fig. 2 with respective peak responsivities of ∼144 and ∼130 mA/W at the wavelength of 265 nm, which correspond to external quantum efficiencies of more than 60%. The responsivities of the MAPDs at long UV wavelengths would be expected to be higher if the 2 μm n$^-$ reach-through layer were depleted. The 4H-SiC diodes exhibit no photoresponse for wavelengths longer than ∼380 nm (see insets of Fig. 2), unlike their 6H counterparts, because of their wider bandgap, and are, therefore, visible-blind.

Figs. 3(a) and 4(a) show the normalized multiplication characteristics of the BAPDs and the MAPDs, respectively, measured using 230–365-nm light. The multiplication characteristics from longer wavelength light are consistently higher than those from light of shorter wavelengths for both structures, with the MAPDs exhibiting a wider spread of multiplication characteristics, as would be expected for a structure with thicker avalanche width. Breakdown voltages of 58.3 and 123.7 V for the BAPDs and the MAPDs, respectively, were also estimated by fitting the multiplication characteristics to Miller's multipli-

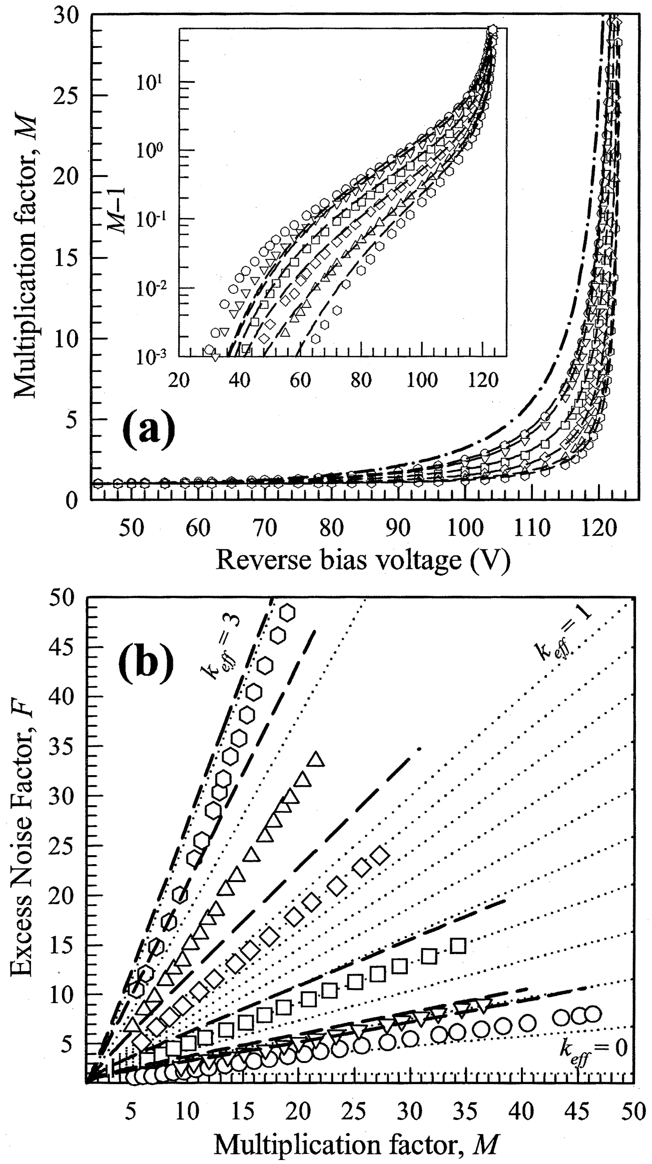

Fig. 4. Measured (symbols) and modeled (dashed lines) (a) multiplication and (b) excess noise characteristics of the MAPD structure from 230 nm (hexagon), 240 nm (△), 250 nm (◇), 265 nm (□), 297 nm (▽), and 365 nm (○). Inset in (a) shows $(M-1)$ plotted on a logarithmic scale to accentuate the low multiplication values. The modeled M_h (dot-dashed line) is also shown in a) for comparison. Dotted lines in (b) are McIntyre's local prediction for $k_{\mathrm{eff}} = 0$ to 1 in steps of 0.1 and $k_{\mathrm{eff}} = 2, 3$.

cation equation [11], in close agreement with results obtained from reverse dark *I–V* measurements.

The excess noise characteristics resulting from carriers injected using 230–365-nm light for the BAPDs and the MAPDs are depicted in Figs. 3(b) and 4(b), respectively. The excess noise measured using 325-nm light from the HeCd laser (not shown) was found to be in good agreement with that measured using the Hg-Xe lamp. The results clearly show that the excess noise of both structures decreases with illuminating wavelength. The lowest excess noise, measured using 365-nm light, corresponds to k_{eff} values of approximately 0.1 and 0.15 in McIntyre's local model [4] for the BAPDs and the MAPDs, respectively. We use a k_{eff} notation to characterize measurements of F as a function of M. Clearly k_{eff} will represent the ratio of ionization coefficients [4] only when dead space effects are negligible.

The weakly absorbed 365-nm light [12] gives a mixed carrier initiated multiplication that is our closest measurable estimate to pure hole multiplication M_h. As the wavelength decreases the UV light is progressively absorbed at shorter depths and more electrons are injected from the top p^+/p cladding layers. It is estimated that more than 95% of the UV light is absorbed in the p^+/p cladding layers of both structures at the wavelength of 230 nm so that the multiplication characteristic from 230-nm light can be considered to correspond to pure electron multiplication M_e. As already pointed out in our earlier work on the BAPDs [5], the behavior of the multiplication characteristics with UV light of various wavelengths shows unambiguously that $\beta > \alpha$. This is further corroborated by the dependence of the multiplication characteristics of the MAPDs and of the excess noise curves of both structures on illumination wavelengths.

The k_{eff} values characterising the excess noise measured with 365-nm light can provide a conservative estimate of the α/β ratio in 4H-SiC within the local approximation if we assume that the excess noise from this wavelength light is due to pure hole injection. In reality, the α/β ratio will be less than this estimate since some electrons from the p^+/p cladding layer are also injected into the avalanche region with the weakly absorbed 365-nm light. Based on this assumption and the local noise model [4] we would expect a lower limit for the excess noise in the BAPDs and MAPDs due to electron injection to correspond to $k_{\mathrm{eff}} \approx 10$ and $k_{\mathrm{eff}} \approx 6.7$, respectively. However, the measured excess noise from electron injection using 230-nm light of the BAPDs and the MAPDs corresponds to much lower values of $k_{\mathrm{eff}} \approx 0.8$ and $k_{\mathrm{eff}} \approx 2.8$, respectively. These values are clearly in disagreement with the lower limits for the electron initiated excess noise of both structures estimated from the characteristics measured with 365-nm light and cannot be explained by the small experimental error (<10%) associated with the excess noise measurements. The discrepancy suggests that dead space effects are important in these structures.

IV. Modeling and Discussion

To help interpret the avalanche multiplication results the responsivity curves of both structures are first modeled using a simple quantum efficiency description to determine the carrier injection profile at each illumination wavelength. A nonlocal model that takes into account the effect of dead space, the carrier injection profile and the nonuniform electric field profile is then used to fit to the measured multiplication and excess noise characteristics of both structures so that the (enabled) ionization coefficients and the ionization threshold energies can be extracted.

A. Quantum Efficiency

The responsivity curves are modeled by treating both APDs as p-i-n structures. This assumption is also reasonable for the MAPDs since the n^- reach-through layer is found to be undepleted from *C–V* and multiplication measurements. For a p-i-n structure, the total photocurrent measured externally is due to i) electrons collected from the p layer at the p-i depletion edge, ii) electron-hole pairs collected from within the depletion region, and iii) holes collected from the n layer at the i-n depletion edge. The internal quantum efficiencies associated with components i)–iii) can be written as [13] [see (1)–(3), shown at the bottom of the page] respectively, where σ is the absorption coefficient at the wavelength λ of the incident light, $L_1(L_2)$ is the minority electron (hole) diffusion length, $D_1(D_2)$ is the electron (hole) diffusion constant, $S_1(S_2)$ is the p(n) layer surface recombination velocity, X_1 is the undepleted width of the p layer, $X_2(X_3)$ is the distance from the front surface to the i$-$n depletion edge (n$^+$ substrate face), and [see (4), shown at the bottom of the page] It is assumed here that all carriers generated within the depletion region are collected. The external quantum efficiency η of the p-i-n structure is then given by

$$\eta = (1-r)(\eta_1+\eta_2+\eta_3) \tag{5}$$

where r is the reflectivity at the front surface. The external quantum efficiency is related to the spectral responsivity by the expression

$$\eta = 1241 \times \frac{R}{\lambda} \tag{6}$$

where R is the responsivity in A/W and λ is the wavelength in nanometers.

The absorption coefficients of 4H-SiC are taken from the work of Sridhara *et al.* [12] for $\lambda > 310$ nm. Those at shorter wavelengths are estimated by extrapolating the data for $\lambda >$ 310 nm and adjusting slightly to fit the responsivity data. The diffusion coefficients of electrons and holes in 4H-SiC are calculated from the electron and hole mobilities, μ_1 and μ_2, respectively, whose values are estimated from [14]. The p cladding thickness of the BAPDs is estimated from the SIMS profile while the nominal value is used for that of the MAPDs. The n cladding thicknesses for both structures were arbitrarily set as 100 μm since the modeled results are found to be insensitive to this parameter. The minority carrier diffusion lengths, the surface recombination velocities (assuming $S_1 = S_2$) and the reflectivity are treated as adjustable parameters. It is noted that the shape of a simulated quantum efficiency curve is most sensitive to the minority carrier diffusion lengths and only a unique combination of L_1 and L_2 can fit the measured results.

TABLE I
PARAMETERS USED TO MODEL THE RESPONSIVITY CURVES OF THE 4H-SiC APDs

Parameters	Units	BAPDs	MAPDs
i-region thickness	μm	0.105	0.285
p cladding thickness	μm	0.45	0.45
n cladding thickness	μm	100	
Electron diffusion length, L_1	μm	1.8	
Hole diffusion length, L_2	μm	1.0	
Electron mobility, μ_1	cm^2/V.s	800	
Hole mobility, μ_2	cm^2/V.s	100	
Surface recombination velocity, assuming $S_1 = S_2$	cm/s	1.2×10^6	
Reflectivity, *r*		~ 0.1	

Table I lists the values of the parameters used in the model to fit the responsivity curves. As shown in Fig. 2, the responsivity curves calculated using these parameters are in good agreement with the measurements. The minority carrier diffusion lengths deduced for 4H-SiC are found to be broadly similar to those of 6H-SiC [15], [16].

B. Avalanche Multiplication

The random path length (RPL) model of Ong *et al.* [17], equivalent [18] to the recurrence model of Hayat *et al.* [19], was used to interpret the measured avalanche multiplication characteristics. This nonlocal model was modified to take into account the distributed carrier injection arising from weakly absorbed UV light and the effect of nonuniform electric field. The ionization behavior of a carrier in a nonuniform electric field region is characterized by the ionization path length probability density function (PDF) $h(x_0, x)$, which describes the probability of the carrier ionizing for the first time after traveling a distance x downstream from the starting position of x_0. In the hard-threshold dead space model the ionization path length PDFs of electrons and holes are

$$\eta_1 = \frac{\sigma L_1}{(\sigma^2 L_1^2 - 1)}\left[\frac{(\sigma D_1 + S_1) - \mathrm{e}^{-\sigma X_1}\left\{S_1\cosh\left(\frac{X_1}{L_1}\right) + \frac{D_1}{L_1}\sinh\left(\frac{X_1}{L_1}\right)\right\}}{S_1\sinh\left(\frac{X_1}{L_1}\right) + \frac{D_1}{L_1}\cosh\left(\frac{X_1}{L_1}\right)} - \sigma L_1 \mathrm{e}^{-\sigma X_1}\right] \tag{1}$$

$$\eta_2 = \mathrm{e}^{-\sigma X_1}\left[1 - \mathrm{e}^{-\sigma(X_2 - X_1)}\right] \tag{2}$$

and

$$\eta_3 = \frac{\sigma L_2 \mathrm{e}^{-\sigma X_2}}{(\sigma^2 L_2^2 - 1)}[\sigma L_2 + K_n] \tag{3}$$

$$K_n = \frac{S_2\left\{\mathrm{e}^{-\sigma(X_3-X_2)} - \cosh\left(\frac{X_3-X_2}{L_2}\right)\right\} - \sigma D_2 \mathrm{e}^{-\sigma(X_3-X_2)} - \frac{D_2}{L_2}\sinh\left(\frac{X_3-X_2}{L_2}\right)}{\frac{D_2}{L_2}\cosh\left(\frac{X_3-X_2}{L_2}\right) + S_2\sinh\left(\frac{X_3-X_2}{L_2}\right)}. \tag{4}$$

given by [20] [see (7), shown at the bottom of the page] for electrons and [see (8), shown at the bottom of the page] for holes where electrons (holes) are assumed to travel in the $x(-x)$ direction, $\alpha^*(z)(\beta^*(z))$ is the position dependent enabled electron (hole) ionization coefficients,$d_e(x_0)(d_h(x_0))$ is the ballistic dead space of the electron (hole) generated at x_0 and w_T is the width of the depletion region.

The ballistic dead space of electrons and holes, $d_e(x_0)$ and $d_h(x_0)$, respectively, can be found by solving the equations

$$q\int_{x_0}^{d_e(x_0)+x_0}\xi(z)dz=E_{the}\quad\text{and}\quad q\int_{x_0-d_h(x_0)}^{x_0}\xi(z)dz=E_{thh} \tag{9}$$

where $\xi(z)$ is the position dependent electric field and $E_{the}(E_{thh})$ is the ionization threshold energy of electrons (holes). The enabled ionization coefficients $\alpha^*(z)$ and $\beta^*(z)$, are related to the effective ionization coefficients, $\alpha(z)$ and $\beta(z)$, by the expressions

$$\frac{1}{\alpha(z)}=de(z)+\frac{1}{\alpha^*(z)}\quad\text{and}\quad\frac{1}{\beta(z)}=d_h(z)+\frac{1}{\beta^*(z)}. \tag{10}$$

Following [17], the probability that an electron and a hole has not ionized after travelling a distance x from x_0 can be written as

$$\mathrm{P_e}(x_0,x)=\exp\left[-\int_{d_e(x_0)}^{x}\alpha^*(z+x_0)dz\right]$$

and

$$\mathrm{P_h}(x_0,x)=\exp\left[-\int_{d_h(x_0)}^{x}\beta^*(x_0-z)dz\right] \tag{11}$$

respectively. The random ionization path length for electron x_e or hole x_h can be determined by equating $\mathrm{P_e}(x_0,x)$ or $\mathrm{P_h}(x_0,x)$ to a random number r such that

$$\int_{d_e(x_0)}^{x_e}\alpha^*(z+x_0)dz=-\ln(r)$$

and

$$\int_{d_h(x_0)}^{x_h}\beta^*(x_0-z)dz=-\ln(r) \tag{12}$$

for electrons and holes, respectively, where $0<r<1$. The integrals in (12) were discretized and implemented as lookup tables to reduce computation time.

Calculation using the RPL model involves simulating many trials (typically>20 000) to build up sufficient statistics to determine M and F from

$$M=\frac{1}{n_\mathrm{T}}\sum_{i=1}^{n_\mathrm{T}}M_i\quad\text{and}\quad F=\frac{1}{n_\mathrm{T}M^2}\sum_{i=1}^{n_\mathrm{T}}M_i^2 \tag{13}$$

where M_i is the multiplication factor from a trial and n_T is the total number of trials. In each trial, carriers are injected at a position determined by the wavelength dependent carrier injection profile deduced from responsivity modeling, where w_T is suitably discretized and n_T is distributed to the spatial mesh of the depletion region according to the calculated profile. A carrier undergoes impact ionization to create a secondary electron-hole pair after travelling a random ionization path length, obtained from (12) using a random number generator, and terminating within the depletion region. This process is repeated for all remaining carriers and the value of M_i is determined from the total number of ionization events when all carriers have left the depletion region.

The electric field profiles are modeled using the parameters extracted from *C–V* measurements. Calculations using the ionization coefficients reported by Konstantinov *et al.* [3] gave much larger breakdown voltages than those measured in both structures. We therefore treat the ionization coefficients as adjustable parameters and obtain initial estimates, parametrized by the expression $\alpha(\beta)=A\exp[-(B/\xi)^c]$, from the multiplication characteristics measured using 230- and 365-nm light by assuming that excitation at 365 nm gives rise to M_h.

The resulting modeled multiplication and excess noise characteristics of the BAPDs and the MAPDs are depicted in Figs. 3 and 4, respectively. The predicted M_h of both structures [see Figs. 3(a) and 4(a)] are observed to be appreciably higher than those measured with 365-nm light, confirming that the β/α ratios are large in these diodes. The multiplication characteristics are also plotted as $(M-1)$ on a logarithmic scale in the insets of Figs. 3(a) and 4(a) to reveal the low multiplication values.

$$h_e(x_0,x)=\begin{cases}0 & \text{for } x<d_e(x_0)\\ \alpha^*(x+x_0)\exp\left[-\int_{d_e(x_0)}^{x}\alpha^*(z+x_0)dz\right] & \text{for } d_e(x_0)\le x\le w_\mathrm{T}-x_0\end{cases} \tag{7}$$

$$h_h(x_0,x)=\begin{cases}0 & \text{for } x<d_h(x_0)\\ \beta^*(x_0-x)\exp\left[-\int_{d_h(x_0)}^{x}\beta^*(x_0-z)dz\right] & \text{for } d_h(x_0)\le x\le x_0\end{cases} \tag{8}$$

The field dependence of the ionization coefficients used in the model can be expressed as

$$\alpha = 1.98 \times 10^6 \exp\left[-\left(\frac{9.46 \times 10^6}{\xi}\right)^{1.42}\right] \text{ cm}^{-1} \quad (14)$$

$$\beta = 4.38 \times 10^6 \exp\left[-\left(\frac{1.14 \times 10^7}{\xi}\right)^{1.06}\right] \text{ cm}^{-1}. \quad (15)$$

Best fits to the measured multiplication and excess noise characteristics of the BAPDs and MAPDs are achieved with ionization threshold values of $E_{the} = 12$ eV and $E_{thh} = 8$ eV. The good agreement between the measured and modeled multiplication curves at low multiplication values in both structures [insets of Figs. 3(a) and 4(a)] provides further evidence that dead space has been properly accounted for. The fitted ionization threshold energies correspond to electron and hole dead spaces that are approximately 28 and 18%, respectively, of the width of a 0.1 μm ideal p-i-n structure at appreciable values of multiplication. We note from the work of Tan *et al.* [21] that a hard-threshold dead space ionization path length PDF predicts higher excess noise than one corresponding to a softer threshold. The small differences between the modeled and measured excess noise curves of both structures may therefore be due to softness of threshold in 4H-SiC.

Fig. 5 shows a comparison of ionization coefficients determined in this work with those reported by Konstantinov *et al.* [3] and Raghunathan and Baliga [6]. As depicted in Fig. 5, the values of β determined from modeling the experimental results are found to agree with the results of Konstantinov *et al.* while our values of α are higher than those of Konstantinov *et al.*, especially at lower fields. In Konstantinov's work ionization coefficients are determined by fitting the local model to the multiplication characteristics of three structures measured using 325-nm light. These authors claimed that the contribution of electrons to multiplication is only significant near breakdown, suggesting that the values of α are critically dependent on the accuracy of the measured data in this region. Multiplication measurements near breakdown are prone to error due to gain saturation effects [22] which can limit the maximum achievable multiplication, especially when high gain and large current are measured. Any resulting error in the measured multiplication near breakdown due to gain saturation effects can translate into significant error in the deduced values of α. Furthermore, the use of only one optical wavelength to measure multiplication and the use of the local model may not be sufficient to determine accurately the ionization coefficients.

Raghunathan and Baliga measured hole initiated multiplication in thick p-type Schottky barrier diodes by generating electron-hole pairs in the depletion region with a pulsed electron beam [6]. In calculating β the measured multiplication characteristics were assumed to be due entirely to hole injection and α was assumed equal to zero. While the second assumption may be appropriate for 4H-SiC, the first assumption may be erroneous since the injection condition is most likely to be mixed due to the significant penetration depth of the electron beam. This could possibly explain the much lower values of β obtained by Raghunathan and Baliga as compared to those of Konstantinov *et al.* and from the present paper.

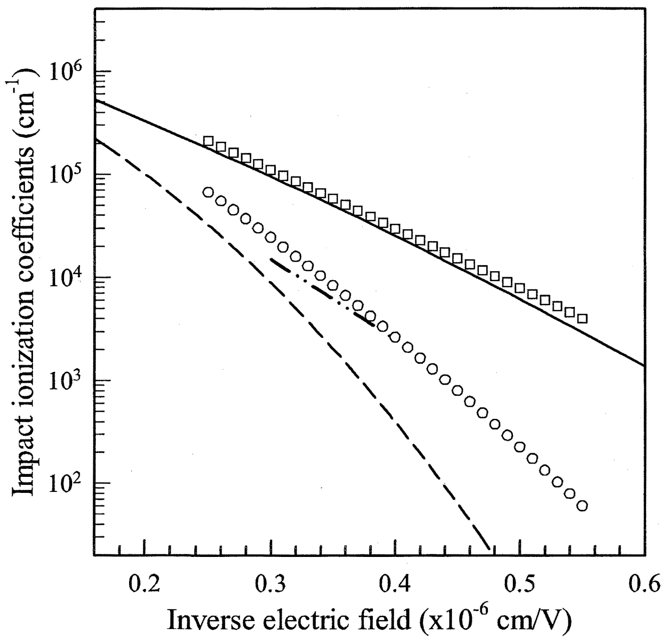

Fig. 5. $\alpha(\bigcirc)$ and $\beta(\square)$ of 4H-SiC obtained in this paper. The results reported by Konstantinov *et al.* (α: dashed line, β: solid line) [3] and Raghunathan and Baliga (β: double dot-dashed line) [6] are also shown for comparison.

V. Conclusion

The avalanche multiplication and excess noise characteristics of 4H-SiC APDs with multiplication region widths of $w = 0.105\ \mu\text{m}$ and $w = 0.285\ \mu\text{m}$ were investigated using 230–365-nm light. Measured multiplication values were found to increase and excess noise to decrease with excitation wavelength. Very low excess noise, corresponding to $k_{\text{eff}} \approx 0.1$ and $k_{\text{eff}} \approx 0.15$ for the $w = 0.105\ \mu\text{m}$ and $w = 0.285\ \mu\text{m}$ APDs, respectively, was measured using 365-nm light. These results show unambiguously that $\beta > \alpha$ and that the β/α ratios remain significantly above unity in these thin 4H-SiC avalanche regions. The multiplication and excess noise characteristics were interpreted using a nonlocal model, in which the wavelength dependent carrier injection profiles and the nonuniform electric field were accounted for. Good agreement with the experimental results was obtained using ionization threshold energies of 12 and 8 eV for electrons and holes, respectively. A small difference between the measured and modeled excess noise suggests that the dead space in 4H-SiC may be soft. The results show that although dead space effects in thin 4H-SiC APDs are important and help to reduce the excess noise, pure hole injection is still necessary to ensure the lowest excess noise because of the persistence of large β/α ratios even at very high fields.

References

[1] K. A. McIntosh, R. J. Molnar, L. J. Mahoney, A. Lightfoot, M. W. Geis, K. M. Molvar, I. Melngailis, R. L. Aggarwal, W. D. Goodhue, S. S. Choi, D. L. Spears, and S. Verghese, "GaN avalanche photodiodes grown by hydride vapor-phase epitaxy," *Appl. Phys. Lett.*, vol. 75, pp. 3485–3487, Nov. 1999.

[2] B. Yang, T. Li, K. Heng, C. Collins, S. Wang, J. C. Carrano, R. D. Dupuis, J. C. Campbell, M. J. Schurman, and I. T. Ferguson, "Low dark current GaN avalanche photodiodes," *IEEE J. Quantum Electron.*, vol. 36, pp. 1389–1391, Dec. 2000.

[3] A. O. Konstantinov, Q. Wahab, N. Nordell, and U. Lindefelt, "Ionization rates and critical fields in 4H silicon carbide," *Appl. Phys. Lett.*, vol. 71, pp. 90–92, Jul. 1997.

[4] R. J. McIntyre, "Multiplication noise in uniform avalanche diodes," *IEEE Trans. Electron Devices*, vol. ED-13, pp. 164–168, 1966.

[5] B. K. Ng, F. Yan, J. P. R. David, R. C. Tozer, G. J. Rees, C. Qin, and J. H. Zhao, "Multiplication and excess noise characteristics of thin 4H-SiC avalanche photodiodes," *IEEE Photon. Technol. Lett.*, vol. 14, pp. 1342–1344, Sept. 2002.

[6] R. Raghunathan and B. J. Baliga, "Temperature dependence of hole impact ionization coefficients in 4H and 6H-SiC," *Solid-State Electron.*, vol. 43, pp. 199–211, 1999.

[7] F. Yan, C. Qin, J. H. Zhao, P. Alexandrov, and M. Weiner, "A novel technology for the formation of a very small bevel angle for high electric field edge termination," in *Tech. Dig. Int. Conf. SiC Related Materials*, Tsukuba, Japan, 2001, pp. 652–653.

[8] F. Yan, Y. Luo, J. H. Zhao, M. Bush, G. H. Olsen, and M. Weiner, "4H-SiC avalanche photodiode with multistep junction extension termination," *Electron. Lett.*, vol. 37, pp. 1080–1081, Aug. 2001.

[9] J. P. Henning, K. J. Schoen, M. R. Melloch, J. M. Woodall, and J. A. Cooper Jr., "Electrical characteristics of rectifying polycrystalline silicon/silicon carbide heterojunctions," *J. Electron. Mater.*, vol. 27, pp. 296–299, 1998.

[10] K. F. Li, D. S. Ong, J. P. R. David, G. J. Rees, R. C. Tozer, P. N. Robson, and R. Grey, "Avalanche multiplication noise characteristics in thin GaAs $\mathrm{p^+ - i - n^+}$ diodes," *IEEE Trans. Electron Devices*, vol. 45, pp. 2102–2107, Oct. 1998.

[11] J. L. Moll, *Physics of Semiconductors*. New York: McGraw-Hill, 1964, pp. 211–238.

[12] S. G. Sridhara, T. J. Eperjesi, R. P. Devaty, and W. J. Choyke, "Penetration depths in the ultraviolet for 4H, 6H and 3C silicon carbide at seven common laser pumping wavelengths," *Mat. Sci. Eng. B*, vol. 61–62, pp. 229–233, 1999.

[13] S. M. Sze, *Physics of Semiconductor Devices*, 2nd ed. New York: Wiley, 1981, pp. 799–805.

[14] A. K. Agarwal, S. S. Mani, S. Seshadri, J. B. Casady, P. A. Sanger, C. D. Brandt, and N. Saks, "SiC power devices," *Naval Res. Rev.*, vol. 51, no. 1, pp. 14–23, 1999.

[15] D. M. Brown, E. T. Downey, M. Ghezzo, J. W. Kretchmer, R. J. Saia, Y. S. Liu, J. A. Edmond, G. Gati, J. M. Pimbley, and W. E. Schneider, "Silicon carbide UV photodiodes," *IEEE Trans. Electron Devices*, vol. 40, pp. 325–333, Feb. 1993.

[16] Y. S. Park, *SiC Materials and Devices of Semiconductors and Semimetals*, R. K. Willardson and E. R. Weber, Eds. New York: Academic, 1998, vol. 52.

[17] D. S. Ong, K. F. Li, G. J. Rees, J. P. R. David, and P. N. Robson, "A simple model to determine multiplication and noise in avalanche photodiodes," *J. Appl. Phys.*, vol. 83, pp. 3426–3428, Mar. 1998.

[18] J. S. Ng, C. H. Tan, B. K. Ng, P. J. Hambleton, J. P. R. David, G. J. Rees, A. H. You, and D. S. Ong, "Effect of dead space on avalanche speed," *IEEE Trans. Electron Devices*, vol. 49, pp. 544–549, Apr. 2002.

[19] M. M. Hayat, B. E. A. Saleh, and M. C. Teich, "Effect of dead space on gain and noise of double-carrier-multiplication avalanche photodiodes," *IEEE Trans. Electron Devices*, vol. 39, pp. 546–552, Mar. 1992.

[20] M. M. Hayat, W. L. Sargeant, and B. E. A. Saleh, "Effect of dead space on gain and noise in Si and GaAs avalanche photodiodes," *IEEE J. Quantum Electron.*, vol. 28, pp. 1360–1365, May 1992.

[21] C. H. Tan, J. P. R. David, G. J. Rees, R. C. Tozer, and D. C. Herbert, "Treatment of soft threshold in impact ionization," *J. Appl. Phys.*, vol. 90, pp. 2538–2543, Sep. 2001.

[22] G. E. Stillman and C. M. Wolfe, "Avalanche photodiodes," in *Semiconductors and Semimetals*, R. K. Willardson and A. C. Beer, Eds. New York: Academic, 1977, vol. 12, pp. 291–393.

B. K. Ng received the B.Eng. and M.Eng. degrees in electrical and electronic engineering from the Nanyang Technological University, Singapore, in 1997 and 2000, respectively. He received the Ph.D. degree in 2003 from the Department of Electronic and Electrical Engineering at the University of Sheffield, Sheffield, U.K., where he investigated the impact ionization process in wide band gap $\mathrm{Al}_x\mathrm{Ga}_{1-x}\mathrm{As}(x > 0.6)$ and SiC for applications in telecommunications and UV avalanche photodiodes.

He is presently a faculty member of the School of Electrical and Electronic Engineering at Nanyang Technological University, Singapore. His research interests include impact ionization process in semiconductors, characterization of avalanche photodiodes and single photon avalanche photodiodes, and biophotonics.

John P. R. David (SM'96) received the B.Eng., and Ph.D. degrees from the Department of Electronic and Electrical Engineering University of Sheffield, Sheffield U.K., in 1979 and 1983, repectively.

In 1983, he joined the Department of Electronic and Electrical Engineering, University of Sheffield, where he worked as a Research Assistant investigating impact ionization. In 1985, he became responsible for characterization within the SERC (now EPSRC) Central Facility for III–V Semiconductors at the same University. Between April 2001 to September 2002, he was at Bookbam Technologies (Caswell) working on III–V material characterization. In September 2002, he returned to faculty position in Sheffield University. His current research interests are low-noise avalanche photodiodes, impact ionization in bulk and multilayer structures and III–V material characterization.

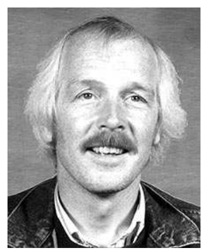

Richard C. Tozer (SM'98) received the B. Eng., M. Eng., and PhD. Degrees from the University of Sheffield, Sheffield, U.K., in 1970 and 1975, respectively.

Following a period of Postdoctoral Research at the University of Sheffield in the area of CCD device applications, he became a Lecturer at the University of Essex, Essex, U.K.,where he researched active sound cancellation. In 1980 he returned as a lecturer to Sheffield where he teaches analog circuit design. His research interests involve the application of analogue circuits to a wide range of experimental and instrumental problem.

Graham J. Rees received degrees in physics and theoretical physics from Oxford University, Oxford, U.K., and Bristol University, Bristol, U.K., respectively.

He has since been with Rome Universita della Scienze, Rome, Italy, Imperial College London, London, U.K., Plessey (now GEC) Caswell, London, Lund University, Lund, Sweden, and Oxford University, Oxford, U.K. He is currently a Professor at the University of Sheffield, Sheffield, U.K. His interests are in the physics of semiconductors and devices.

Feng Yan (SM'97) was born in Taiyuan, China in 1968. He received the B.S. and M.S. degrees from the Department of Physics from Nanjing University, Nanjing, China in 1990 and 1993, respectively. He joined the Department of Electrical and Computer Engineering at Rutgers University, Piscataway, NJ, since 1997 as a Ph.D student. His thesis work is focused on developing 4H-SiC avalanche photodiodes.

He was with Department of Physics, Nanjing University from 1993 to 1996, working on Si-based nanometer semiconductors and devices. He has worked at the NASA Goddard Space Flight Center since 2002. His current interest is on semiconductor detector development. He has published over 40 journal papers.

Jian H. Zhao (SM'94) received the B.S. degree in physics from Xiamen University, Xiamen, China, in 1982, the M.S. degree in physics from the University of Toledo, Toledo, OH, in 1985, and the Ph.D. degree in electrical engineering from Carnegie Mellon University, Pittsburgh, PA, in 1988.

He joined Rutgers University, Piscataway, NJ in 1988 as an Assistant Professor and is currently Professor and Director of SiCLAB, Department of Electrical and Computer Engineering. His research interests include wide bandgap semiconductor electronic and optoelectronic devices, III–V photonic devices, waveguide devices, and device modeling. He has authored and coauthored more than 120 refereed journal papers, four book chapters, and a book *Optical Filter Design and Analysis: A Signal Processing Approach* (New York: Wiley, 1999). He has eight patents awarded or pending.

Maurice Weiner (F'92) received the Ph.D. degree in physics from New York University, New York, NY in 1971.

In 1961, he joined the U.S. Army Research Laboratory, Fort Monmouth, NJ, where he was engaged in the development of microwave ferrite and gaseous electronic devices. Later, as Leader of the Solid State Pulsers Team, he led the development of optically activated semiconductors, thyristors, and other solid state devices. In 1998, he joined United Silicon Carbide, Inc., North Brunswick, NJ, where he has helped to develop research programs for a variety of silicon carbide devices. He is the author of *Electromagnetic Analysis Using Transmission Line Variables* (Singapore: World Scientific, 2001).

Dr. Weiner served on numerous scientific panels and organized several workshops related to high-power semiconductor devices. He was Chairman of the 1994 IEEE Power Modulator Conference and served as coeditor of a Special Issue on the IEEE TRANSACTIONS ON ELECTRON DEVICES (December 1990), devoted to optically controlled semiconductor devices. He received the U.S. Army Research and Development Award in 1984, 1988, and 1992.